

“Research Note”

**VERTEX BASE UNSTRUCTURED FINITE VOLUME SOLUTION OF DEPTH
AVERAGED TURBULENT TIDAL CURRENTS ON 3D BED***

S. R. SABBAGH-YAZDI AND M. ZOUNEMAT-KERMANI**

Dept. of Civil Engineering, K.N.Toosi University of Technology, Tehran, I. R. of Iran
Email: SYazdi@kntu.ac.ir

Abstract– In the present paper, simulations of tidal currents in the Persian Gulf using depth average flow solver version of NASIR (Numerical Analyzer for Scientific and Industrial Requirements) software are verified. The hydrodynamic equations utilized in this work consist of depth integrated equations of continuity and motion in two dimensional horizontal planes (SWE). The effects of rainfall-evaporation are considered in the continuity equation and the effects of bed slope and friction, as well as the Coriolis effects are considered in two equations of motion. The vertex base finite volume method is applied for solving the governing equations on triangular unstructured meshes. Due to the complexity of the coastal boundaries and the existence of irregularly shaped islands, turbulent flow circulations may play an effective role in the formation of flow field parameters. Therefore, the effect of turbulent modelling on the accuracy of the depth averaged circulating flow simulation is investigated. The performance of the computer model to simulate tidal flow in the Persian Gulf domain is examined by imposing tidal fluctuations to the main flow boundary during a limited period of time. In addition, in order to illustrate the computed tidal flow characteristics in the Persian Gulf, an S_2 tidal constituents chart is presented.

Keywords– Tidal circulating flow, Persian Gulf, unstructured grid, finite volumes method

1. INTRODUCTION

The availability of high performance computers and the development of efficient numerical modelling techniques have led to the development of powerful Computational Fluid Dynamics (CFD) models for the solution of fluid flow cases [1]. Moreover, the computer simulation of complicated marine environment problems has become one of the interesting areas of research works by development of efficient and accurate numerical methods suitable for the complex flow domain.

Three-dimensional flow solvers are accurate, but computationally expensive due to the required number of elements and numerical techniques for modelling time dependent water flow problems. Two-dimensional depth average models are well-established models where the vertical velocity components are not significant in comparison with the horizontal components [2-4]. Hence, it seems that such conditions match most areas of the Persian Gulf region (with 1000 km length, 340 km maximum width and less than 0.1 km maximum depth). Therefore, two-dimensional tidal currents may be modelled by a depth averaged hydrodynamic model.

Several numerical workers tried to model the hydrodynamic behaviour of the Persian Gulf. Some of the numerical models of the Persian Gulf reported in the literature have used two-dimensional depth averaged hydrodynamic equations in a Cartesian coordinates system [5, 6]. In order to get more accurate results, in some modelling efforts, the two-dimensional depth averaged equations are transformed into a spherical coordinates system [7, 8].

*Received by the editors September 5, 2005; Accepted May 19, 2008.

**Corresponding author

A numerical model is not able to simulate the real world flow pattern unless the geometrical characteristics of the flow domain (i.e. the irregularities of coasts and islands) are properly modelled. Thus, the numerical flow solver should handle the geometrical complexities of the bed and boundaries.

In order to overcome the problem, an attempt has made to solve the depth averaged hydrodynamic equations on unstructured finite volumes. The flow solver is tested for simulation of circulating flows in deep waters, and then it is applied to model tidal currents in the Persian Gulf.

2. HYDRODYNAMIC EQUATIONS

The convection-diffusion equation, which is formed by both transport and diffusion terms, is applied to model the transient depth average currents. The depth averaged equations (Shallow Water Equations) are chosen as the governing equation of the flow in the Persian Gulf. The governing equations are written in vector form as follows:

$$\frac{\partial W}{\partial t} + \left(\frac{\partial F^c}{\partial x} + \frac{\partial G^c}{\partial y} \right) = \left(\frac{\partial F^d}{\partial x} + \frac{\partial G^d}{\partial y} \right) + S, \quad W = \begin{pmatrix} h \\ hu \\ hv \end{pmatrix}, \quad F^c = \begin{pmatrix} hu \\ hu^2 \\ huv \end{pmatrix}, \quad G^c = \begin{pmatrix} hv \\ huv \\ hv^2 \end{pmatrix},$$

$$F^d = \begin{pmatrix} 0 \\ hv_{th} 2 \left(\frac{\partial u}{\partial x} \right) \\ hv_{th} \left(\frac{\partial v}{\partial x} + \frac{\partial u}{\partial y} \right) \end{pmatrix}, \quad G^d = \begin{pmatrix} 0 \\ hv_{th} \left(\frac{\partial u}{\partial y} + \frac{\partial v}{\partial x} \right) \\ hv_{th} 2 \left(\frac{\partial v}{\partial y} \right) \end{pmatrix}, \quad S = \begin{pmatrix} q_z \\ -gh \frac{\partial \eta}{\partial x} + hv f_c - \frac{\tau_{bx}}{\rho_w} + \frac{\tau_{wx}}{\rho_w} \\ -gh \frac{\partial \eta}{\partial y} - hv f_c - \frac{\tau_{by}}{\rho_w} + \frac{\tau_{wy}}{\rho_w} \end{pmatrix} \quad (1)$$

Where, W represents the conserved variables using h flow depth, u and v the horizontal components of velocity, G^c and F^c are vectors of convective fluxes while, G^d and F^d are vectors of diffusive fluxes of W in x and y directions, respectively. The vector S contains the source and sink terms of the governing equations [9].

Using the above equations, the currents in the Persian Gulf are computed considering q_z the rainfall-evaporation from the unit area of the water surface, surface and bed slopes $\eta = h + z_b$, global bed friction stresses $\tau_{bx} = \rho_w C_f u |U|$ and $\tau_{by} = \rho_w C_f v |U|$ ($C_f = gn^2 / h^{0.33}$ using n manning coefficient), global wind stresses on water surface $\tau_{wx} = \rho_{air} C_w u_{wx} |V_{wind\ 10m}|$ and $\tau_{wy} = \rho_{air} C_w v_{wy} |V_{wind\ 10m}|$ (with $C_w = 0.001$), Coriolis forces $f_c = \omega \sin \phi$ (using ω earth angular velocity and ϕ the geographical latitude of the point).

In the present work, two algebraic types of turbulent models are examined for computation of eddy viscosity parameter ν_{th} . First, the widely used depth-averaged parabolic model has been utilised (in which the eddy viscosity parameter is computed using the following algebraic formulation)

$$\nu_{th} = C_p h U_* \quad (2)$$

Where the empirical coefficient C_p was taken as 0.1 [10]. In the above formulation the bed friction velocity is defined as, $U_* = [C_f (u^2 + v^2)]^{0.5}$. The other applied turbulent model is recognised as a kind of Sub-Grid Scale turbulent model, namely the SGS model [11, 12]. In the SGS model, the eddy viscosity parameter can be calculated using the following equation.

$$\nu_{th} = C_s^2 \Delta^2 \sqrt{S_{xy} S_{xy}} \quad (3)$$

Where C is a constant and taken to be 0.1 to 1.0, Δ^2 represents the grid size which can be consigned by the area of the calculated cell in unstructured grids. The S_{ij} is the tensor form and can be calculated by the following equation [13, 14].

$$S_{xy} = \left(\frac{\partial u}{\partial y} + \frac{\partial v}{\partial x} \right) \quad (4)$$

3. FINITE VOLUME MODEL

Through application of the finite volume method, the governing equation is converted into discrete form by integrating over a control volume Ω .

$$\frac{\partial}{\partial t} \int_{\Omega} W d\Omega + \int_{\Omega} \left(\frac{\partial}{\partial x} F^c + \frac{\partial}{\partial y} G^c \right) d\Omega = \int_{\Omega} \left(\frac{\partial}{\partial x} F^d + \frac{\partial}{\partial y} G^d \right) d\Omega + \int_{\Omega} S d\Omega \quad (5)$$

By application of the Gauss-Divergence theorem, the volume integral of convective and diffusive fluxes are converted to boundary integrals as

$$\frac{\partial}{\partial t} \int_{\Omega} W d\Omega + \int_{\Gamma} (F^c dy - G^c dx) = \int_{\Gamma} (F^d dy - G^d dx) + \int_{\Omega} S d\Omega \quad (6)$$

Where W_o represents conserved variables at the centre of control volume Ω_o . In the over-lapping vertex base finite volume method a control volume is formed by gathering cells sharing a nodal point.

In the above formulation \bar{F}^c and \bar{G}^c are the mean values of convective fluxes on the control volume boundary sides. The parameters \tilde{F}^d and \tilde{G}^d are diffusive fluxes which include gradients of velocity components. In the current research, the Galerkin finite volume method was chosen for computing \tilde{F}^d and \tilde{G}^d . The Galerkin finite volume method is formulated by multiplying the linear shape function of triangular elements to the weak form of the governing equations and integrating over a vertex base control volume Ω_o .

Considering all the triangular cells as one Ω control volume, Eq. (6) can be rewritten as:

$$\Omega \frac{dW}{dt} = \sum_{k=1}^{N_{side}} \left(\frac{F_{j1}^c + F_{j2}^c}{2} \right)_k \vec{\Delta} l_k - \sum_{k=1}^{N_{side}} \frac{3}{2} (F_A^d) \vec{\Delta} l_k \quad (7)$$

Here, $\vec{\Delta} l_k$ represents the normal edge length of the face of each triangle opposite of i node on edge k and A is the area of a secondary control volume in which the diffusive fluxes are computed at its centre.

4. BOUNDARY CONDITIONS

Two types of flow boundary and wall boundary conditions are applied in this work. As for flow boundaries, the tidal flow boundary condition is considered by imposing water surface level fluctuations. For the Persian Gulf, the fluctuations of water surface elevation at Didamar Island (near Hormouz Strait) can be obtained by application of the calibrated constants of the harmonic analysis for any arbitrary period of time (Admiralty Tide Tables [15]). Moreover, the Arvand river inflow is imposed whenever the inside domain water surface level is less than the water level at the flow boundary (Report on Rainfall and surface currents in Iran [16]).

On behalf of wall boundaries, although small water depths in coastal zones rise to the global bed shear stresses and reduce the computed velocities, tangential velocity reduction coefficient may be used to model the effect of these boundaries. A no-slip boundary condition must be implemented where the wall

boundary friction has a considerable effect on the flow regime. At these boundaries all velocity components are set to zero.

5. VERIFICATION TESTS

The hydrodynamic model is examined for circulating shallow (friction dominated) and deep (frictionless) flows in two channels with sudden expansion. The accuracy of the results is assessed by comparison between the numerical results and the reported measurements in the literature.

The first channel with sudden expansion in its right wall is a well known frictionless test case. In this case, the bed friction effect is negligible. The channel width is $2m$ before and $3m$ after the expansion section. Before the expansion part of the channel the mean velocity is $0.5m/s$ and the flow depth $1m$ [16].

The second test case is a bed friction dominated flow in a channel with sudden expansion. The channel width is $0.305m$ before and $0.71m$ after the expansion section. Before the expansion part of the channel the mean velocity is $0.145m/s$ and the flow depth $0.0819m$ [17]. A discretized domain and sample of flow patterns in terms of streamlines for two cases are shown in Figs. 1 and 2.

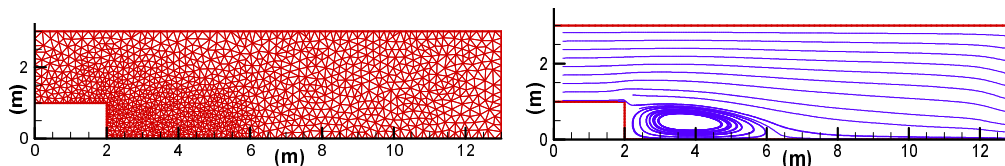


Fig. 1. Left: The discretized domain of the frictionless channel expansion; Right: Stream lines and recirculation region

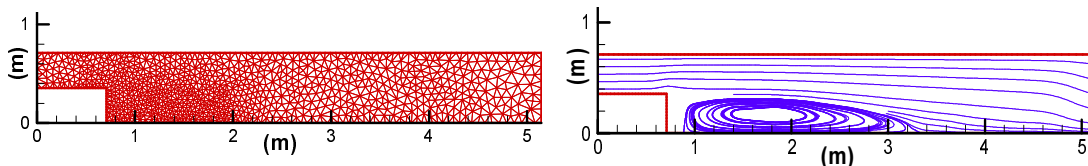


Fig. 2. Left: The discretized domain of the side-wall expansion friction dominated channel; Right: Stream lines and recirculation region

The computed results of recirculation length after the sudden expansion of the above mentioned test cases for various bed friction and turbulent modelling conditions are tabulated in Table 1.

Table 1. Comparison of computed recirculation length using depth averaged algebraic eddy viscosity turbulent models with measured data for two test cases

	Frictionless case		Friction dominated case	
	measurement	Error	measurement	Error
Experimental measurement	3.95(m)	---	2.40(m)	---
No turbulent model ($\nu_{th} = 0$)	4.10(m)	3%	3.30(m)	37%
Parabolic model ($\nu_{th} = C_p h U_*$)	4.10(m)	3%	2.50(m)	4%
SGS model ($\nu_{th} = C_s^2 \Delta^2 \sqrt{S_{xy} S_{xy}}$)	4.00(m)	1%	3.15(m)	31%

In the frictionless flow test case, zero value is considered for the roughness coefficient (C_f). Thereafter, using a depth-averaged parabolic model which uses $U_* = [C_f(u^2 + v^2)]^{0.5}$ does not play any role in formation of the flow circulation. Although the SGS model result shows better agreement to experimental measurement, there is no considerable difference between the three conditions of zero, depth-averaged parabolic and SGS eddy viscosity turbulent models for the case of negligible bed friction.

In the friction dominated test case, the best recirculation length after the channel expansion is obtained by application of the depth-averaged parabolic model. Due to light computational work load and the acceptable performances, particularly for the shallow water turbulent flows in the regions with considerable bed friction, the depth-averaged parabolic model was selected as a favourite turbulent model for the computation of tidal circulations in the Persian Gulf.

6. PERSIAN GULF FLOW SIMULATION

Here, the numerical simulation of currents in the Persian Gulf is presented after evaluation of the accuracy of the developed hydrodynamic model.

Horizontal geometry of the problem is modelled by definition of 1060 boundary curves which represent coastal boundaries and eight major islands. Then, the flow domain is discretized using unstructured mesh generated by the Deluaney Triangulation Technique [18]. The Persian Gulf mesh, which contains 7288 nodes, 13532 elements, and 20828 edges (Fig. 3), is refined at flow boundaries and close to the islands using point and line sources for mesh spacing.

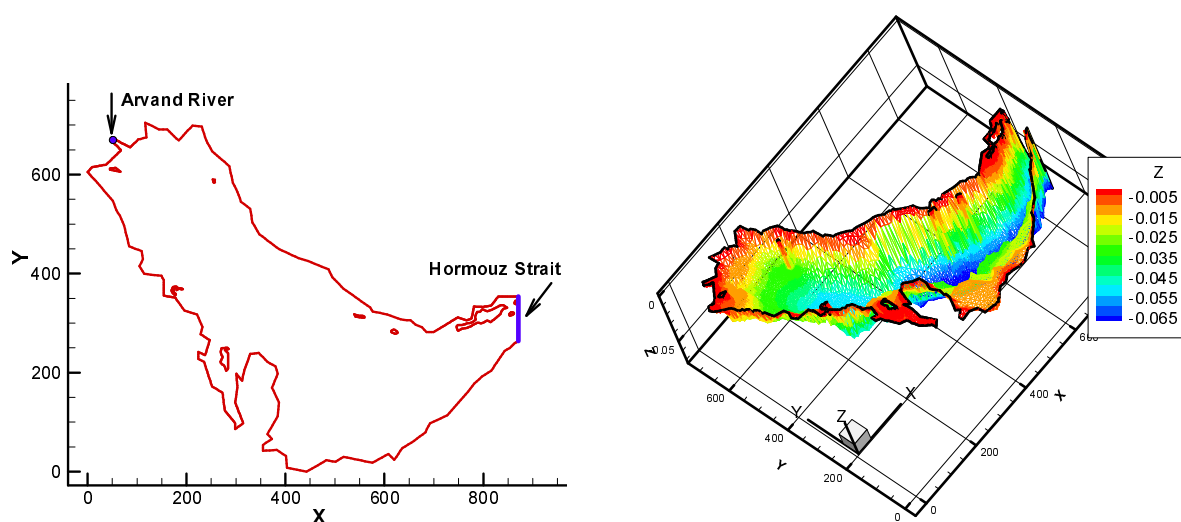


Fig. 3. Left: boundary conditions for present numerical modelling of the Persian Gulf; Right: 3D Bottom surface formed by triangular mesh (dimensions in kilometres)

The described hydrodynamic model is used to compute flow patterns in the Persian Gulf due to tidal fluctuations at the east boundary, river inflow at the west coast, evaporations from water surface, Coriolis effect, friction and irregularities of coasts and bed (using unstructured three dimensional surface mesh). In order to verify the quality of the results, the tidal fluctuations at Didamar island, obtained from the Admiralty Tide Table for the period of 12 days from December 2003 are imposed at the Hormouz Strait (the east end of the flow domain). The inflow from the Arvand River (located at the border line between IRAN and IRAQ) is imposed at the end the estuary located at the north west of the flow domain. Considering the evaporations from the water surface and Coriolis effects, the flow patterns are formed due to the coasts and bed geometry and roughness. Typical results of surface water elevation and streamlines in an arbitrary time are depicted in Fig. 4. Also, the water surface elevation computed by the hydrodynamic model is compared with the predictions of the Admiralty Tide Table at the port of Bushehr (Fig. 5)

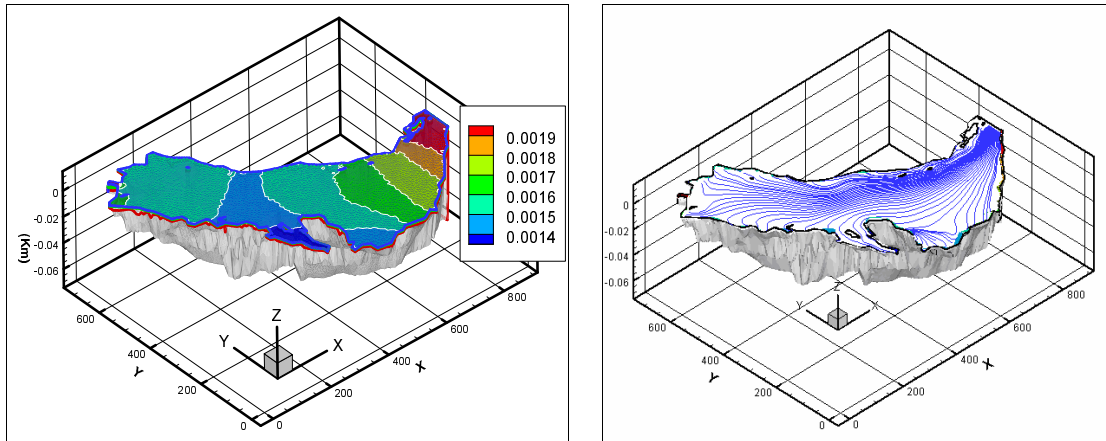


Fig. 4. Sample computed colour coded maps of water surface elevation (Right) and stream traces (Left) in an arbitrary time

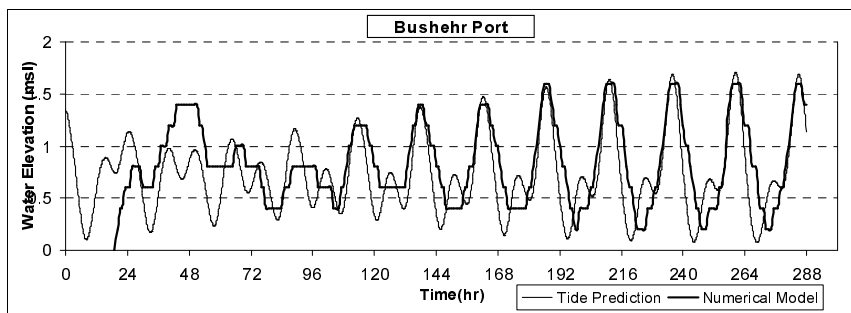


Fig. 5. Comparison of computed water surface level fluctuations with Admiralty Tide Table prediction at Bushehr port (Verification point of the model)

In order to make a global verification on tidal results, S_2 tidal constituents were produced from the computed results of the present model. S_2 represents principal solar semidiurnal with a period of 12.00hr [18]. Fast Fourier Transform (FFT) [19] is utilized for producing the following plots (Fig. 6).

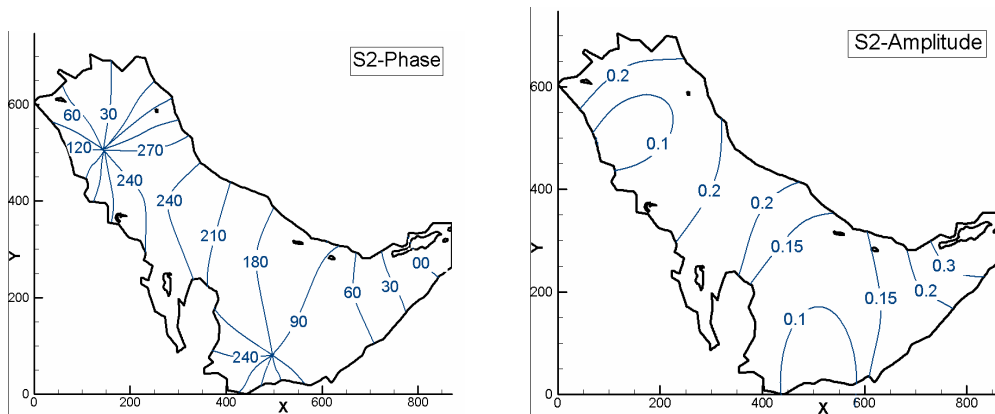


Fig. 6. Amplitude (m) and phase (deg) maps of S_2 tidal constituent in the Persian Gulf

7. CONCLUSION

The depth averaged flow solver module is successfully utilized to simulate the tidal currents in the Persian Gulf. The computed two dimensional circulations by two types of algebraic turbulent models (depth-averaged parabolic model and SGS model) as well as non-turbulent flow were compared with the reported measurements of two test cases. The SGS model produced good results for the flow regions with

negligible bed friction effects, but it failed to produce accurate results in the regions where bed friction is pronounced. Hence, the application of the depth averaged parabolic turbulent model is considered for the tidal flow modelling of the Persian Gulf, due to the existence of shallow water regions with considerable bed friction. Considering tidal fluctuations at the Hormouz Strait flow boundary, inflow from the Arvand river, evaporations and Coriolis effects, three-dimensional bottom surface geometry, coastal and island boundaries and bed roughness, the tidal flow patterns in the Persian Gulf are successfully modelled.

REFERENCES

1. Karimian, S. M. H., Amoli, A. & Mazaheri, K. (2002). Control-volume finite-element method for the solution of 2d euler equations on unstructured moving grids. *Iranian Journal of Science and Technology, Transaction B*, Vol. 26, No. B3, pp. 465-476.
2. Talebbeydokhti, N. & Ghotb, M. R. (2001). Finite element modeling of flows in open channels transitions. *Iranian Journal of Science and Technology, Transaction B*, Vol. 25, No. B3, pp. 669-680.
3. Sabbagh-Yazdi, S. R. & Mohammad Zadeh Qomi, M. (2004). Finite volume solution of two-dimensional convection dominated sub-critical flow using unstructured triangular meshes. *International Journal of Civil Engineering*, Vol. 2, No. 2, pp. 78-91.
4. Sabbagh-Yazdi, S. R. & Zounemat-Kermani, M. (2007). Numerical investigation of island effects on depth averaged fluctuating flow in the Persian Gulf. *International Journal of Engineering, Transactions A: Basics*, Vol. 20, No. 2, pp. 117-128.
5. Von-Trepka, L. (1968). Investigation of the tides in the Persian Gulf by means of a hydrodynamic numerical model. in *Proceeding of Symposium on Mathematical Hydrological Investigations of Physical Process in the Sea, Inst. Fur Meer. Der Univ. Hamburg*, Vol. 10, pp. 59-63.
6. Chu, W. S., Baker, B. L. & Akbar, A. M. (1988). Modelling tidal transport in Arabian Gulf. *Journal of Water Way, Port, Coastal and Ocean Engineering*, Vol. 114, pp. 455-471.
7. Hunter, J. R. (1984). Tidal and stratification-mixing models of Kuwait waters. *Kuwait Bulletin of Marin Science*, Vol. 5, pp. 11-35.
8. Najafi, H. S., Noye, B. J. & Teubner, M. D. (1995). Spherical-coordinate numerical model of the Persian Gulf. *Computational Techniques and Applications, CTAC-95*, World Scientific.
9. Vreugdenhil, C. B. (1994). *Numerical methods for shallow water flow*. Kluwer Academic Publisher.
10. Rodi, W. (1993). *Turbulence models and their applications in hydraulics*. 3rd Edition, IAHR Monograph, Balkema, Rotterdam, Netherlands.
11. Gallerano, F. & Napoli, E. (2000). Balance equation of the generalised sub-grid scale (SGS) turbulent kinetic energy in a new tensorial dynamic mixed SGS model. *Continuum Mechanics Thermodynamics*. Vol. 12, pp. 79-94.
12. Smagorinsky, J. (1963). General circulation experiments with the primitive equations, Part I: The basic experiment. *Monthly Weather Review*, Vol. 91, pp. 99-152.
13. Li, C. W. & Wang, J. H. (2000). Large eddy simulation of free surface shallow-water flow. *International Journal for Numerical Methods in Fluids*, Vol.34, pp. 31-46.
14. Murakami, S. (1993). Comparison of various turbulence models applied to a bluff body. *Journal of wind Engineering and Industrial Aerodynamics*, Vol. 46&47, pp. 21-36.
15. Admiralty Tide Tables, (1964). British Admiralty.
16. Report on Rainfall and Surface Currents in Iran, (2003). Water Resource Management Organization of Iran (Farsi).
17. Denham, M. K. & Patrick, M. A. (1974). Laminar flow over a downstream facing step in a two dimensional flow channel, *Trans. Inst. Chemical Engineers*, Vol. 52, pp. 361-367.

18. Babaruis, S., Ganoulis, J. & Chu, V. H. (1989). Experimental investigation of shallow recirculating flows. *J. of Hyd. Div. ASCE*, Vol. 115, pp. 906-924.
19. Weatherill, N. P. (1996). A review of mesh generation. Special Lecture, *Advances in Finite Element Technology*, Civil-Comp press. Edinbrough, pp. 1-10.
20. Shurman, P. (1958). Manual of harmonic analysis and prediction of tides. Reprinted.
21. Pawlowicza, R., Beardsley, B. & Lentz, S. (2002). Classical tidal harmonic analysis including error estimates in MATLAB. *Computers and Geosciences*, Vol. 28, pp. 929-937.